Supporting Information

Ti_3C_2 MXene cocatalyst supported $Ti_3C_2/SrTiO_3/g\text{-}C_3N_4$ heterojunctions with efficient electron transfer for photocatalytic H_2 production

Xiaoyun Ye[a, *], Hangyu Zhong[a], Yumei Zhang[a], Xuehua Liu[a], Wei Tian[b], Li-An Ma[a, *], Qianting Wang[a, c, *]

[a] College of Materials Science and Engineering, Fujian University of Technology, 33 South Xuefu Road, Fuzhou 350118, China

[b] College of Ecological Environment and Urban Construction, Fujian University of Technology, 33 South Xuefu Road, Fuzhou 350118, China

[c] School of Materials Science and Engineering, Xiamen University of Technology, Xiamen, 361024, China

*Corresponding author.

Email address: creekye@163.com (X. Ye); mlajn@163.com (L. Ma); wqt@xmut.edu.cn (Q. Wang)

Table S1 The experimental parameters of the samples

Sample	Ti_3C_2 (mg)	TiO_2 (mg)	$Sr(NO_3)_2$ (mg)	$Ti_3C_2/SrTiO_3$ (mg)	g-C_3N_4 (mg)	Reaction time (h)	Roasting temperature（℃）
$SrTiO_3$	-	40	105.8	-	-	4	140
MS	137.6	40	105.8	-	-	4	140
MSCN-20	0	0		120	30	2	200
MSCN-40	0	0		120	80	2	200
MSCN-60	0	0		120	180	2	200
MSCN-80	0	0		120	480	2	200

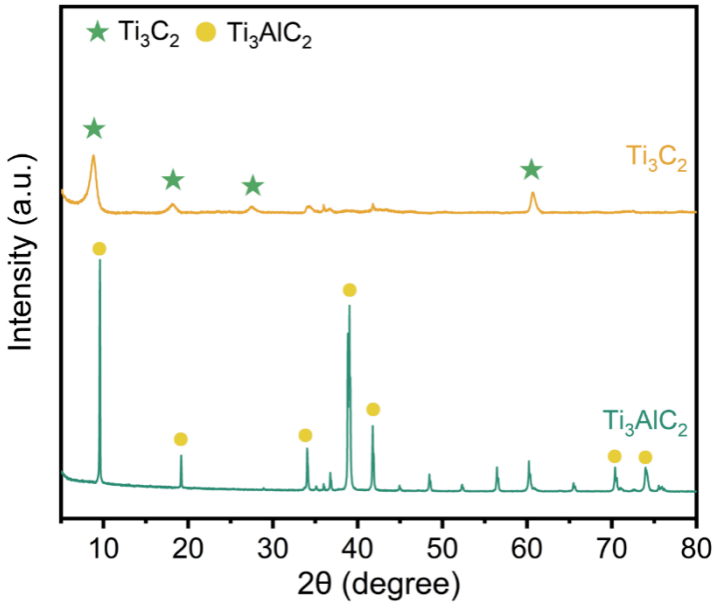

Fig. S1 XRD patterns of Ti_3AlC_2 and Ti_3C_2

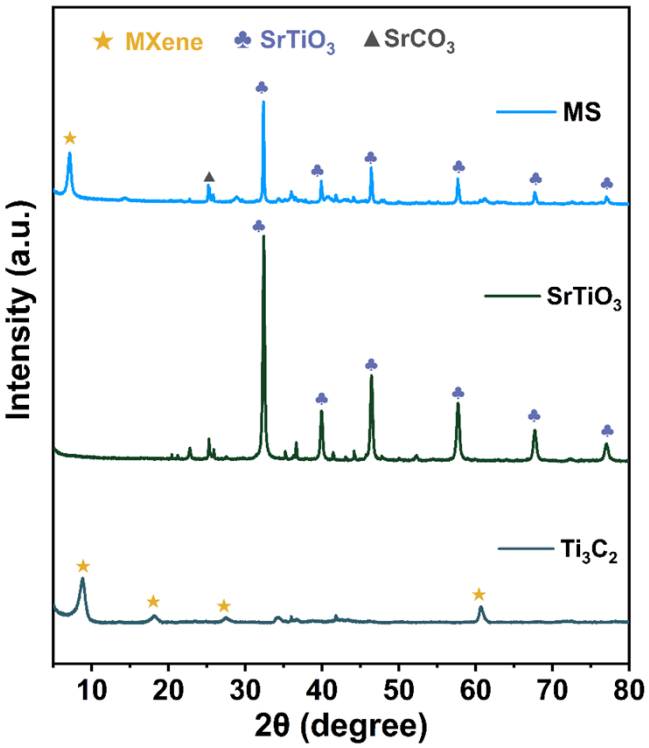

Fig. S2 XRD patterns of Ti_3C_2, $SrTiO_3$ and MS

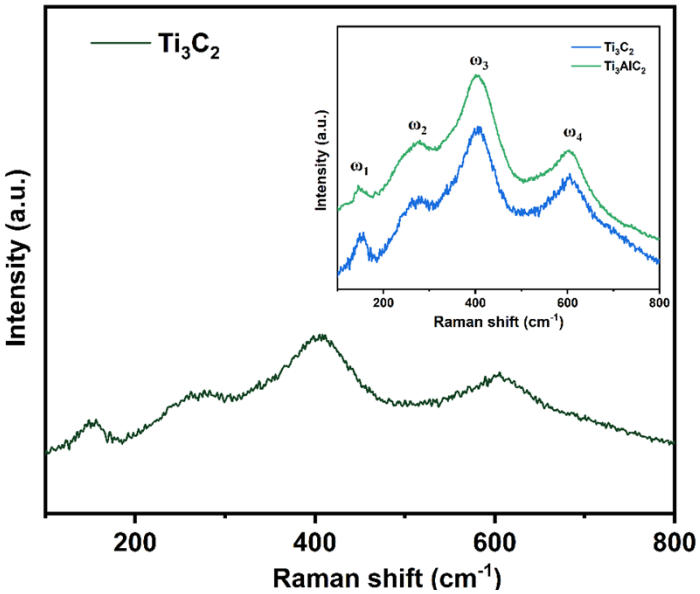

Fig. S3 Raman spectra of Ti_3C_2

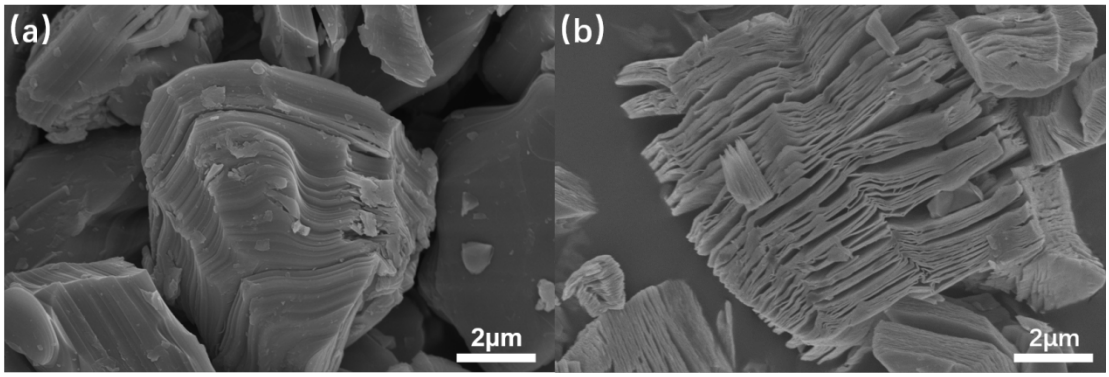

Fig. S4 SEM images of (a) Ti_3AlC_2, (b) Ti_3C_2

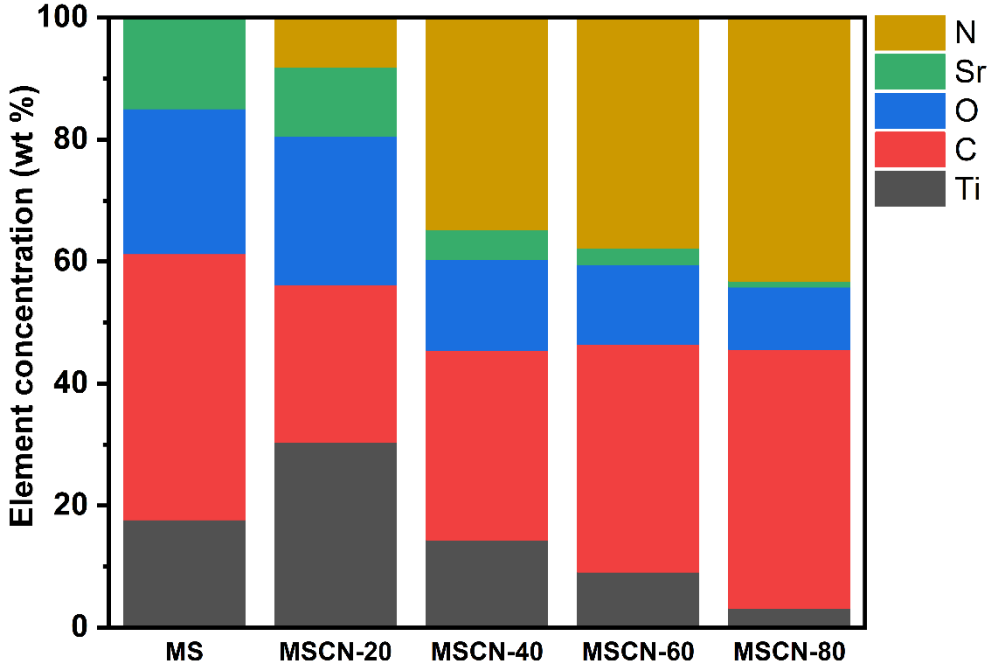

Fig. S5 The quantitative analysis of MSCN-60

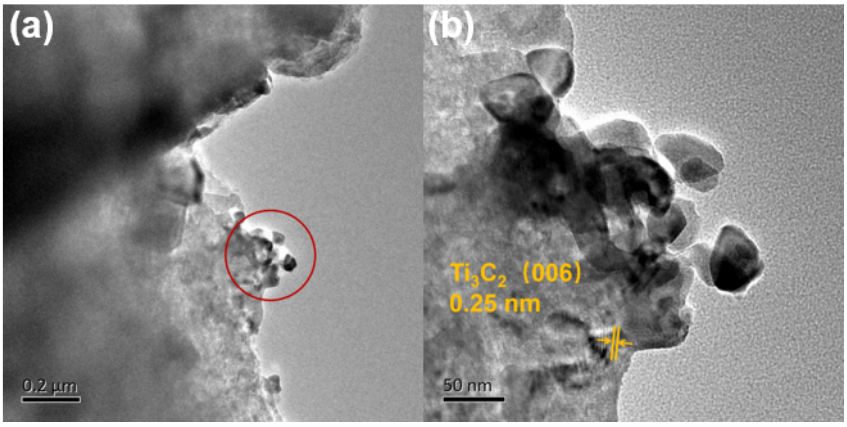

Fig. S6 TEM images of the MS

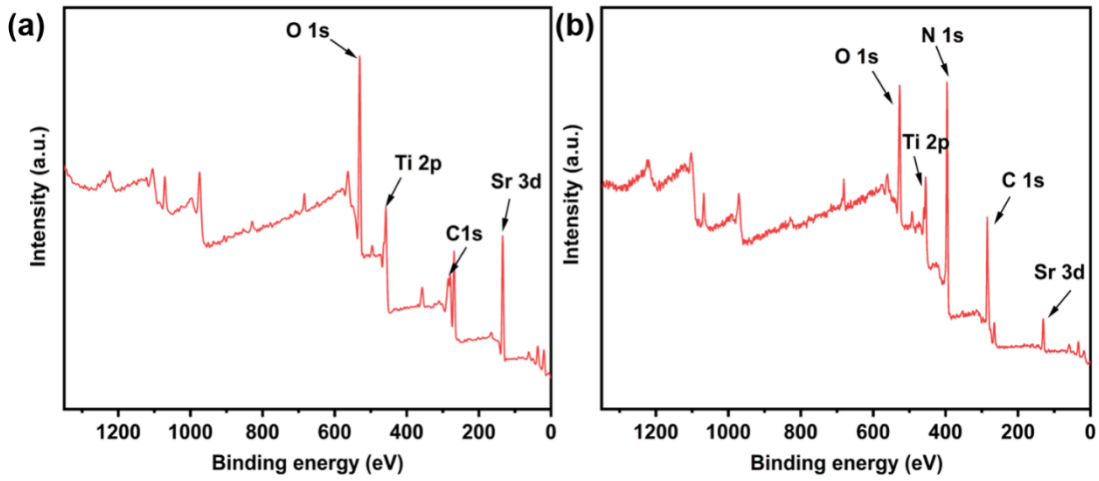

Fig. S7 XPS full spectra of (a) MS, (b) MSCN-60

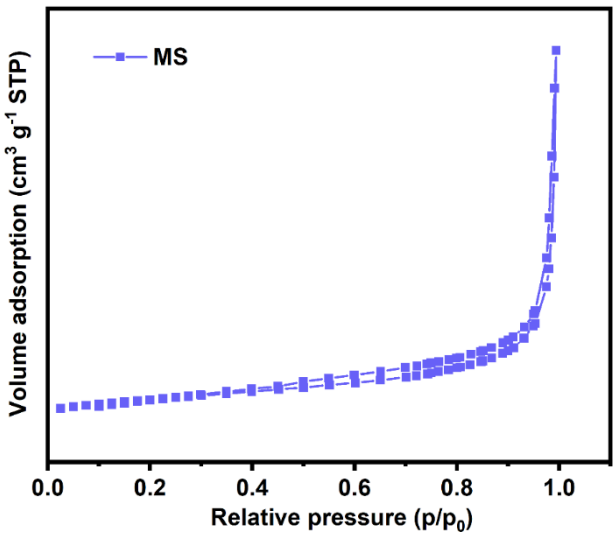

Fig. S8 N_2 isothermal adsorption-desorption curves of the MS

Table S2 Specific surface area and pore volume data of the samples

Samples	S_{BET} (m^2/g)	$^{\alpha}$PV (cm^3/g)
MS	8.05	3.41
MSCN-20	14.79	0.09
MSCN-40	6.96	0.06
MSCN-60	5.70	0.09
MSCN-80	10.15	0.09

$^{\alpha}$PV: void volume

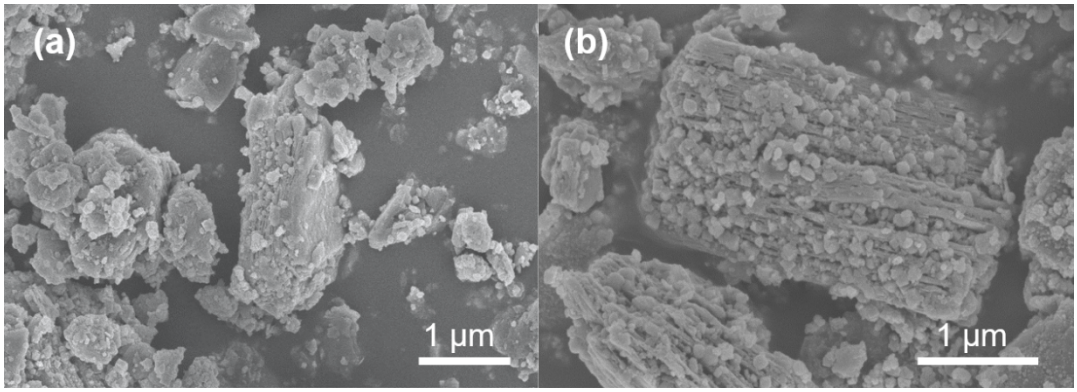

Fig. S9 SEM images of MSCN-60

Table S3 The performance comparison of this work and the related photocatalysts

Photocatalyst	Light source	Performance ($\mu mol \cdot g^{-1} \cdot h^{-1}$)	Year	Reference
$TiO_2/Ti_3C_2/g\text{-}C_3N_4$	visible light	2592	2021	[48]
$Ti_3C_2/R\text{-}TiO_2$	simulated sunlight	0.00162	2023	[49]
$Ti_3C_2/TiO_2/rGO$	simulated sunlight	417.96	2022	[50]
$TiO_2\{001\}/g\text{-}C_3N_4$	visible light	1780	2021	[51]
$Au/SrTiO_3/TiO_2$	visible light	327.4	2022	[52]
$C\text{-}TiO_2/g\text{-}C_3N_4$	visible light	1409	2020	[53]
Cu_2O/TiO_2	simulated sunlight	1388.13	2022	[54]
$N_2\text{-}TiO_2$	visible light	103.6	2023	[55]
MSCN-60	simulated sunlight	1733.13	2024	This work

2.4 Materials characterization

The samples were characterized morphologically and structurally characterized by field emission scanning electron microscopy (FESEM, NANO-VASEM 450, FEI) and transmission electron microscopy (TEM, JEM-2100, JEOL). The crystal structures of the samples were characterized by X-ray powder diffraction (XRD, D8-ADVANCE, BRUKER) under Cu-Kα radiation (λ = 1.54056 Å) at a scanning rate of 6 °/min in the 2θ range from 5 ° to 80 °. A Raman spectrometer (Thermo Fisher Scientific DXRxi) was used, excited by a 663 nm laser was used. Composition and elemental distribution were observed by energy dispersive spectroscopy (EDS, OXFORD). Electron binding

energy, elemental valence and surface composition were analyzed by X-ray photoelectron spectroscopy (XPS, ESCALAB 250Xi) using an Al-Kα X-ray source. N_2 adsorption-desorption curves were recorded on a 3Flex 3500 analyzer (Micromeritics ASAP 2020, USA) to measure the surface area and pore volume of the samples. The fluorescence spectrometer (FLS980, Edinburgh Instruments) was used to measure the time-resolved PL decay curves. The absorption capacity of the samples was analyzed on a UV-Vis diffuse reflectance spectrophotometer (SHIMADZU UV-3600 Plus) using $BaSO_4$ as a standard material. Electrochemistry impedance spectroscopy (EIS) and photocurrent intensity response measurements with a 300 W Xe lamp were performed on an electrochemical workstation (CS310H, Corrtest) based on a conventional three electrode cell, where a sample-coated clean fluoride-tin oxide (FTO) glass, Pt plate and a Calomel electrode were used as the working electrode, counter electrode (CE) and reference electrode (RE), respectively. The aqueous solution of 0.5 M Na_2SO_4 purged with nitrogen gas was used as the electrolyte.

Photocatalytic hydrogen evolution test: The photocatalytic hydrogen evolution test was performed in a 100 mL quartz glass reactor. 20 mg of the composite photocatalyst was dispersed in 20 mL of a 20 vol% methanol aqueous solution (in the photocatalytic reaction, an amount of H_2PtCl_6 solution was added to the reaction solution, and 3 wt% of Pt was in-situ deposited on the photocatalyst as a co-catalyst), which was then transferred to a quartz container. Prior to the illumination experiments, the interior of the reactor was evacuated to ensure a vacuum environment. A 300 W Xe lamp (MC-PF300C, Beijing Merry Change Technology Co., Ltd.) was selected as the

light source. The reaction system was illuminated with the full solar spectrum and circulating cooling water was used to maintain the entire reactor temperature at a constant 25 °C with a reaction time of 4 h. The reaction system was kept under constant agitation to ensure uniform irradiation of the catalyst suspension during the experimental process. Using pure argon as the carrier gas, a gas chromatograph (GC9790II, Zhejiang Fuli Analytical Instrument Co., Ltd.) was used to analyze the composition of the gas produced. The molar amount of hydrogen produced per unit mass of photocatalyst per unit time was calculated as an evaluation criterion of the activity of the photocatalyst.